# Biomimetic amplification of nanoparticle homing to tumors

Dmitri Simberg, Tasmia Duza, Ji Ho Park, Markus Essler, Jan Pilch, Lianglin Zhang, Austin M. Derfus, Meng Yang, Robert M. Hoffman, Sangeeta Bhatia, Michael J. Sailor, and Erkki Ruoslahti

*PNAS* published online Jan 10, 2007;
doi:10.1073/pnas.0610298104

# Biomimetic amplification of nanoparticle homing to tumors

Dmitri Simberg[a], Tasmia Duza[a,b], Ji Ho Park[c,d], Markus Essler[a,e], Jan Pilch[a], Lianglin Zhang[a], Austin M. Derfus[a,f], Meng Yang[g], Robert M. Hoffman[g,h], Sangeeta Bhatia[i,j], Michael J. Sailor[c,d], and Erkki Ruoslahti[a,k,l]

[a]Cancer Research Center, Burnham Institute for Medical Research, 10901 North Torrey Pines Road, La Jolla, CA 92037; [k]Burnham Institute for Medical Research at University of California Santa Barbara, 1105 Life Sciences Technology Building, University of California, Santa Barbara, CA 93106-9610; [c]Department of Chemistry and Biochemistry, University of California at San Diego, 9500 Gilman Drive, La Jolla, CA 92093-0358; [d]Materials Science and Engineering Program, University of California at San Diego, 9500 Gilman Drive, La Jolla, CA 92093-0418; [f]Department of Bioengineering, University of California at San Diego, 9500 Gilman Drive, La Jolla, CA 92093-0412; [g]AntiCancer, Inc., 7917 Ostrow Street, San Diego, CA 92111; [h]Department of Surgery, University of California, 200 West Arbor Drive, San Diego, CA 92103-8820; [i]Harvard–Massachusetts Institute of Technology Division of Health Sciences and Technology, 77 Massachusetts Avenue, Cambridge, MA 02139; and [j]Department of Electrical Engineering and Computer Science, Massachusetts Institute of Technology/Brigham and Women's Hospital, 75 Francis Street, Boston, MA 02115

Contributed by Erkki Ruoslahti, November 22, 2006 (sent for review November 13, 2006)

**Nanoparticle-based diagnostics and therapeutics hold great promise because multiple functions can be built into the particles. One such function is an ability to home to specific sites in the body. We describe here biomimetic particles that not only home to tumors, but also amplify their own homing. The system is based on a peptide that recognizes clotted plasma proteins and selectively homes to tumors, where it binds to vessel walls and tumor stroma. Iron oxide nanoparticles and liposomes coated with this tumor-homing peptide accumulate in tumor vessels, where they induce additional local clotting, thereby producing new binding sites for more particles. The system mimics platelets, which also circulate freely but accumulate at a diseased site and amplify their own accumulation at that site. The self-amplifying homing is a novel function for nanoparticles. The clotting-based amplification greatly enhances tumor imaging, and the addition of a drug carrier function to the particles is envisioned.**

clotting | liver | peptide | tumor targeting | iron oxide

Nanomedicine is an emerging field that uses nanoparticles to facilitate the diagnosis and treatment of diseases. Notable early successes in the clinic include the use of superparamagnetic nanoparticles as a contrast agent in MRI and nanoparticle-based treatment systems (1, 2). The first generation of nanoparticles used in tumor treatments rely on "leakiness" of tumor vessels for preferential accumulation in tumors; however, this enhanced permeability and retention is not a constant feature of tumor vessels (3) and, even when present, still leaves the nanoparticles to negotiate the high interstitial fluid pressure in tumors (3, 4). An attractive alternative would be to target nanoparticles to specific molecular receptors in the blood vessels because they are readily available for binding from the blood stream and because tumor vessels express a wealth of molecules that are not significantly expressed in the vessels of normal tissues (5–7).

Specific targeting of nanoparticles to tumors has been accomplished in various experimental systems (8–10), but the efficiency of delivery is generally low. In nature, amplified homing is an important mechanism, ensuring sufficient platelet accumulation at sites of vascular injury. Amplified homing involves target binding, activation, platelet–platelet binding, and formation of a blood clot. We have designed a nanoparticle delivery system in which the particles amplify their own homing in a manner that resembles platelets.

## Results

**CREKA Peptide.** We used a tumor-homing peptide to construct targeted nanoparticles. We identified this peptide by *in vivo* screening of phage-displayed peptide libraries (5, 11) for tumor homing in tumor-bearing MMTV-PyMT transgenic breast cancer mice (12). The most frequently represented peptide sequence in the selected phage preparation was CREKA (Cys-Arg-Glu-Lys-Ala). We synthesized the CREKA peptide with a fluorescent dye attached to the N terminus and studied the *in vivo* distribution of the peptide in tumor-bearing mice. Intravenously injected CREKA peptide was readily detectable in the PyMT tumors, and in MDA-MB-435 human breast cancer xenografts, minutes to hours after the injection. The peptide formed a distinct meshwork in the tumor stroma [supporting information (SI) Fig. 5*A*], and it also highlighted the blood vessels in the tumors. The CREKA peptide was essentially undetectable in normal tissues. In agreement with the microscopy results, whole-body imaging using CREKA peptide labeled with the fluorescent dye Alexa Fluor 647 revealed peptide accumulation in the breast cancer xenografts and in the bladder, reflecting elimination of excess peptide into the urine (SI Fig. 5*B*).

Tumors contain a meshwork of clotted plasma proteins in the tumor stroma and the walls of vessels, but no such meshwork is detectable in normal tissues (13–15). The mesh-like pattern produced by the CREKA peptide in tumors prompted us to study whether clotted plasma proteins might be the target of this peptide. We tested the peptide in fibrinogen knockout mice, which lack the fibrin meshwork in their tumors. Like previously identified clot-binding peptides (15), intravenously injected CREKA peptide failed to accumulate in B16F1 melanomas grown in the fibrinogen null mice but formed a brightly fluorescent meshwork in B16F1 tumors grown in normal littermates of the null mice (Fig. 1 *A* and *B*). In agreement with this result, the CREKA phage, but not the control insertless phage, bound to clotted plasma proteins *in vitro* (Fig. 1*C*). These results establish CREKA as a clot-binding peptide. Its structure makes it an attractive peptide to use in nanoparticle targeting because, unlike our other clot-binding peptides, which are cyclic 10 amino acid peptides (15), CREKA is linear and contains only 5 aa. Moreover, the sulfhydryl group of the single cysteine residue is

Author contributions: D.S., T.D., and E.R. designed research; D.S., T.D., J.H.P., M.E., J.P., L.Z., A.M.D., and M.Y. performed research; J.H.P. and R.M.H. contributed new reagents/analytic tools; D.S., T.D., J.H.P., M.E., J.P., L.Z., A.M.D., M.Y., R.M.H., S.B., M.J.S., and E.R. analyzed data; and D.S. and E.R. wrote the paper.

The authors declare no conflict of interest.

Abbreviations: RES, reticuloendothelial system; SPIO, superparamagnetic, amino dextran-coated iron oxide; SQUID, superconducting quantum interference device.

[b]Present address: Berlex, Inc., 6 West Belt, Wayne, NJ 07470-6806.

[e]Present address: Nuklearmedizinische Klinik und Poliklinik Ismaningerstrasse 22, 81675 Munich, Germany.

[l]To whom correspondence should be addressed. E-mail: ruoslahti@burnham.org.

This article contains supporting information online at www.pnas.org/cgi/content/full/0610298104/DC1.

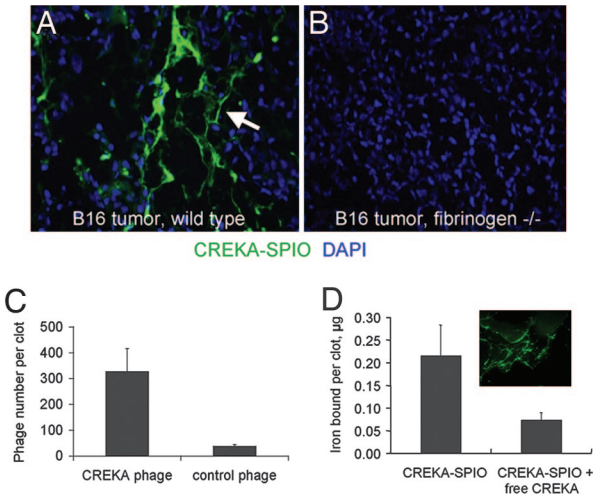


**Fig. 1.** Tumor homing of CREKA pentapeptide. (*A* and *B*) Fluorescein-conjugated CREKA peptide (200 $\mu$g per mouse) was injected into mice bearing syngeneic B16F1 melanoma tumors. Representative microscopic fields are shown to illustrate homing of fluorescein-CREKA to fibrin-like structures in tumors in wild-type mice (*A*, arrow) and lack of homing in fibrinogen null mice (*B*). (*C*) The CREKA phage binds to clotted plasma proteins in a test tube, whereas nonrecombinant control phage shows little binding. (*D*) Dextran-coated iron oxide nanoparticles conjugated with fluorescein-CREKA bind to clotted plasma proteins, and the binding is inhibited by free CREKA peptide. (*D Inset*) The microscopic appearance of the clot-bound CREKA-SPIO. [Magnification: ×200 (*A* and *B*) and ×600 (*D Inset*).]

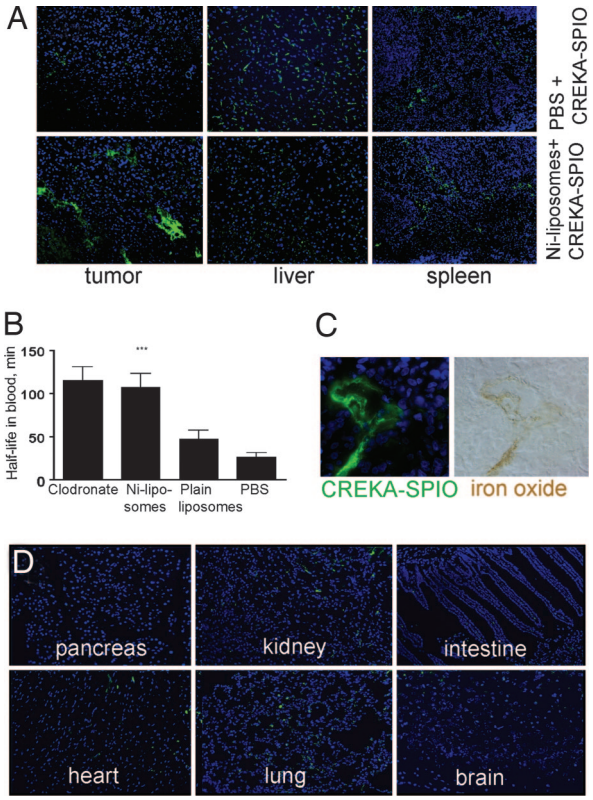


**Fig. 2.** Tumor homing of CREKA-conjugated iron oxide particles. CREKA-SPIO particles were intravenously injected (4 mg of Fe per kg) into BALB/c nude mice bearing MDA-MB-435 human breast cancer xenograft tumors measuring 1–1.5 cm in diameter. The mice were killed by perfusion 5–6 h later, and tissues were examined for CREKA-SPIO fluorescence (green). Nuclei were stained with DAPI (blue). (*A*) Distribution of CREKA-SPIO in tissues from MDA-MB-435 tumor mice that 2 h earlier had received an injection of PBS (*Upper*) or Ni/DSPC/CHOL liposomes (Ni-liposomes) containing 0.2 $\mu$mol Ni in 200 $\mu$l of PBS (*Lower*). (*B*) Plasma circulation half-life of CREKA-SPIO after different treatments. At least four time points were collected. Data were fitted to monoexponential decay by using Prizm software (GraphPad, San Diego, CA), and the half-life values were compared in unpaired *t* test (***, $P < 0.0001$ relative to PBS control; $n = 10$). (*C*) Accumulation of CREKA-SPIO nanoparticles in tumor vessels. Mice were injected and tissues were collected as in *A*. Fluorescent intravascular CREKA-SPIO particles overlap with iron oxide viewed in transmitted light. (Magnification: ×600.) (*D*) Control organs of Ni-liposome/CREKA-SPIO-injected mice. Occasional spots of fluorescence are seen in the kidneys and lungs. The fluorescence seen in the heart did not differ from uninjected controls, indicating that it is autofluorescence. Representative results from at least three independent experiments are shown. [Magnification: ×200 (*A* and *D*) and ×600 (*C*).]

not required to provide binding activity and can be used to couple the peptide to other moieties.

**Peptide-Coated Nanoparticles.** We coupled fluorescein-labeled CREKA or fluorescein onto the surface of 50-nm superparamagnetic, amino dextran-coated iron oxide (SPIO) nanoparticles. Such particles have been extensively characterized with regard to their chemistry, pharmacokinetics, and toxicology and are used as MRI contrast agents (16–18). Coupling of the fluorescein-labeled peptides to SPIO produced strongly fluorescent particles. Releasing the peptide from the particles by hydrolysis increased the fluorescence further by a factor of ≈3 (data not shown). These results indicate that the proximity of the fluorescein molecules at the particle surface causes some quenching of the fluorescence. Despite this quenching, fluorescence from the coupled fluorescein peptide was almost linearly related to the number of peptide molecules on the particle (SI Fig. 6), allowing us to track the number of peptide moieties on the particle by measuring particle fluorescence and to use fluorescence intensity as a measure of the concentration of particles in samples. We used CREKA-SPIO with at least 8,000 peptide molecules per particle in our *in vivo* experiments. The CREKA-SPIO nanoparticles bound to mouse and human plasma clots *in vitro*, and the binding was inhibited by the free peptide (Fig. 1*D*). The nanoparticles distributed along a fibrillar meshwork in the clots (Fig. 1*D Inset*). These results show that the particle-bound peptide retains its binding activity toward clotted plasma proteins.

**Tumor Homing vs. Liver Clearance of CREKA-SPIO.** Initial experiments showed that intravenously injected CREKA-SPIO nanoparticles did not accumulate effectively in MDA-MB-435 breast cancer xenografts. In contrast, a high concentration of particles was seen in reticuloendothelial system (RES) tissues (Fig. 2*A Upper*). Because the free CREKA peptide effectively homes to these tumors (SI Fig. 5), we hypothesized that the RES uptake was a major obstacle to the homing of the nanoparticles. We confirmed the role of the RES in the clearance of CREKA-SPIO by depleting RES macrophages in the liver with liposomal clodronate (19). This treatment caused an ≈5-fold prolongation in particle half-life (Fig. 2*B*). Particulate material is eliminated from the circulation, because certain plasma proteins bind to the particles and mediate their uptake by the RES (opsonization) (20, 21). Injecting decoy particles that eliminate plasma opsonins is another commonly used way of blocking RES uptake (22, 23). We tested liposomes coated with chelated $Ni^{2+}$ as a potential decoy particle because we surmised that iron oxide and $Ni^{2+}$ would attract similar plasma opsonins, and Ni-liposomes could therefore deplete them from the systemic circulation. Indeed, SDS/PAGE analysis showed that significantly less plasma protein bound to SPIO in the blood of mice that had been pretreated with Ni-liposomes (results not shown).

Intravenously injected Ni-liposomes prolonged the half-life of

the SPIO and CREKA-SPIO in the blood by a factor of ≈5 (Fig. 2*B*). The Ni-liposome pretreatment, whether done 5 min or 48 h before the injection of CREKA-SPIO, greatly increased the tumor homing of the nanoparticles, which primarily localized in tumor blood vessels (Fig. 2 *A Lower* and *D*). The local concentration of particles could be so high that the brownish color of iron oxide was visible in the optical microscope (Fig. 2*C Right*), indicating that the fluorescent signal observed in tumor vessels was from intact CREKA-SPIO. Fewer particles were seen in the liver after the Ni-liposome pretreatment, but accumulation in the spleen was unchanged or even enhanced (Fig. 2*A*). Other organs contained minor amounts of CREKA-SPIO particles or no particles at all, whether Ni-liposomes were used or not (Fig. 2*D*). Although Ni-liposomes were quite effective, they caused some deaths in the tumor mice, prompting us to also test plain liposomes as decoy particles. These liposomes prolonged the blood half-life and tumor homing of subsequently injected CKEKA-SPIO (Fig. 2*B* and data not shown), suggesting the existence of a common clearance mechanism for liposomes and SPIO. However, although the plain liposomes showed no apparent toxicity, they were less effective as decoy particles than the Ni-liposomes. Reducing the Ni content of the liposomes may provide a suitable compromise between toxicity and efficacy.

**Nanoparticle-Induced Blood Clotting in Tumor Vessels.** CREKA-SPIO particles administered after liposome pretreatment primarily colocalized with tumor blood vessels, with some particles appearing to have extravasated into the surrounding tissue (Fig. 3*A Top*). Significantly, up to 20% of tumor vessel lumens were filled with fluorescent masses. These structures stained for fibrin (Fig. 3*A Middle*), suggesting that they are blood clots impregnated with nanoparticles. In some of the blood vessels, the CREKA-SPIO nanoparticles were distributed along a meshwork (Fig. 3*A Middle Inset*), presumably formed of fibrin and associated proteins, and similar to the pattern shown in Fig. 1*D Inset*.

Among the non-RES tissues, the kidneys and lungs contained minor amounts of specific CREKA-SPIO fluorescence (Fig. 2*D*). However, low-magnification images, which reveal only blood vessels with clots in them, showed no clotting in these tissues, with the exception of very rare clots in the kidneys (SI Fig. 7). Despite massive accumulation of nanoparticles in the liver, we saw no colocalization between fibrin(ogen) staining and CREKA-SPIO fluorescence in liver vessels (SI Fig. 8). Moreover, liver tissue from a noninjected mouse also stained for fibrin(ogen) (SI Fig. 8*B*), presumably reflecting fibrinogen production by hepatocytes. Thus, the clotting induced by CREKA-SPIO nanoparticles is essentially confined to tumor vessels.

Nanoparticles can cause platelet activation and enhance thrombogenesis (24, 25). Some CREKA-SPIO nanoparticles (<1%) recovered from blood were associated with platelets (SI Fig. 9*A*), but staining for a platelet marker showed no colocalization between the platelets and CREKA-SPIO nanoparticles in tumor vessels (Fig. 3*A Bottom*). We also induced thrombocytopenia by injecting mice with an anti-CD41 monoclonal antibody (26) and found no noticeable effect on CREKA-SPIO homing to the MDA-MB-435 tumors (SI Fig. 9*B*). These results indicate that platelets are not involved in the homing pattern of CREKA-SPIO.

The deep infiltration of clots by nanoparticles suggested that these clots must have formed at the time particles were circulating in blood rather than before the injection. We tested this hypothesis with intravital confocal microscopy, using DiI-labeled erythrocytes as a flow marker. There was time-dependent clot formation and obstruction of blood flow in tumor blood vessels with parallel entrapment of CREKA-SPIO in the forming clots (Fig. 3*B*; and see SI Movie 1).

We next tested whether the clotting-inducing effect was specific for SPIO particles, or could be induced with a different

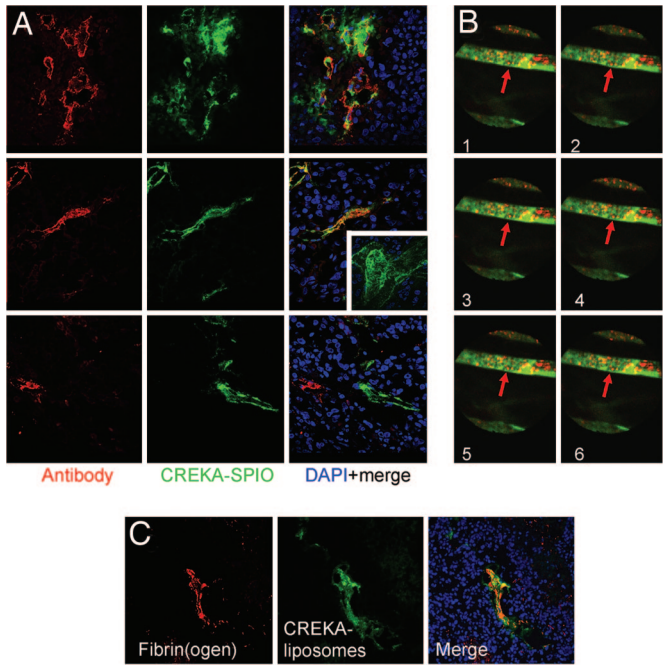


**Fig. 3.** Accumulation of CREKA-SPIO nanoparticles in tumor vessels. Mice bearing MDA-MB-435 xenografts were injected with Ni-liposomes and CREKA-SPIO nanoparticles as described in the legend to Fig. 2. The mice were perfused 6 h after the nanoparticle injection, and tissues were collected. (*A Top*) Colocalization of nanoparticle fluorescence with CD31 staining in blood vessels. (*A Middle*) Colocalization of nanoparticle fluorescence and antifibrin(ogen) staining in tumor blood vessels. (*Inset*) An image showing CREKA-SPIO distributed along fibrils in a tumor blood vessel. (*A Bottom*) Lack of colocalization of nanoparticle fluorescence with anti-CD41 staining for platelets. (*B*) Intravital confocal microscopy of tumors using DiI-stained red blood cells as a marker of blood flow. The arrow points to a vessel in which stationary erythrocytes indicate obstruction of blood flow. Blood flow in the vessel above is not obstructed. Six successive frames from a 1-min movie (SI Movie 1) are shown. (*C*) CREKA-coated liposomes colocalize with fibrin in tumor vessels. The results are representative of three independent experiments. [Magnification: ×600 (*A* and *C*) and ×200 (*B*).]

CREKA-coated particle. We used liposomes into which we incorporated fluorescein-CREKA peptide that was coupled to lipid-tailed polyethylene glycol. Like CREKA-SPIO, the CREKA-liposomes selectively homed to tumors and colocalized with fibrin within tumor vessels (Fig. 3*C*), suggesting that CREKA liposomes are also capable of causing clotting in tumor vessels. No clotting was seen when control SPIO or control liposomes were injected in the tumor mice.

**Clotting-Amplified Tumor Targeting.** We next studied the contribution of clotting to the accumulation of CREKA-SPIO in tumor vessels. Quantitative analysis of tumor magnetization with a superconducting quantum interference device (SQUID) (Fig. 4*A*), and measurement of the fluorescence signal (data not shown) revealed ≈6-fold greater accumulation of CREKA-SPIO in Ni-liposome-pretreated mice compared with PBS-pretreated mice. Aminated SPIO control particles did not significantly accumulate in the tumors (Fig. 4*A*).

The SQUID measurements revealed that injecting heparin, which is a strong clotting inhibitor, before injection of CREKA-SPIO reduced tumor accumulation of nanoparticles by >50% (Fig. 4*A*). Microscopy showed that heparin reduced the fibrin-positive/CREKA-SPIO-positive structures within tumor vessels but that the particles still bound along the walls of the vessels, presumably to preexisting fibrin deposits (a representative image is shown in Fig. 4*B*). Separate quantification of the homing

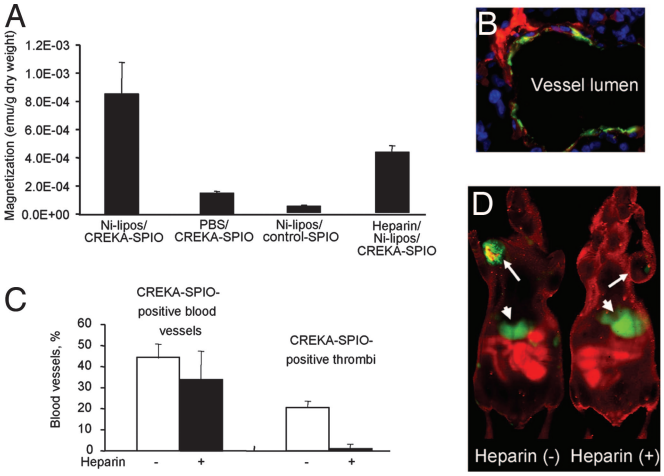


**Fig. 4.** Effect of blood clotting on nanoparticle accumulation in tumors. Mice bearing MDA-MB-435 human breast cancer xenografts were intravenously injected with PBS or a bolus of 800 units/kg of heparin, followed 120 min later by Ni-liposomes (or PBS) and CREKA-SPIO (or control nanoparticles). The mice received additional heparin by i.p. injections (a total of 1,000 units/kg) or PBS throughout the experiment. (*A*) Tumors were removed 6 h after the nanoparticle injection, and magnetic signal in the tumor after different treatments was determined with SQUID. Aminated dextran SPIO served as a particle control (control SPIO). SPIO nanoparticle concentration in tissues is represented by the saturation magnetization value (electromagnetic unit, emu) of the tissue at 1T magnetic field after the subtraction of the diamagnetic and the paramagnetic background of blank tissue. The magnetization values were normalized to dry weight of the tissue. Results from three experiments are shown. (*B*) Quantification of heparin effect on clotting in blood vessels. Mice were pretreated with PBS (open bars) or heparin (filled bars) as described above, followed by Ni liposomes/CREKA-SPIO nanoparticles. Three sections from two tumors representing each treatment were stained with anti-CD31 for blood vessels, and the percentage of vessels positive for fluorescence and fluorescent clots was determined. Note that heparin did not significantly change the percentage of blood vessels containing particles, but dramatically decreased the incidence of the lumens that are filled with fluorescence. (*C*) A representative example of the appearance of CREKA-SPIO particles in tumor vessels of mice treated with heparin. (*D*) Near-infrared imaging of mice that received Ni-liposomes, followed by Cy7-labeled CREKA-SPIO, with or without heparin pretreatment. The images were acquired 8 h after the injection of the CREKA-SPIO particles by using an Odyssey 2 NIR scanner (Li-COR Biosciences, Lincoln, NE). The images shown are composites of two colors, red (700-nm channel, body and chow autofluorescence) and green (800-nm channel, Cy7). Arrows point to the tumors, and arrowheads point to the liver. Note the strong decrease in signal from the tumor in the heparin-pretreated mouse. One representative experiment of three is shown.

pattern showed that heparin did not significantly reduce the number of vessels with nanoparticles bound to the vessel walls, but essentially eliminated the intravascular clotting (Fig. 4*C*). Thus, the binding of CREKA-SPIO to tumor vessels does not require the clotting activity that is associated with these particles, but clotting improves the efficiency of the tumor homing.

The clotting induced by CREKA-SPIO caused a particularly strong enhancement of tumor signal in whole-body scans. CREKA-SPIO nanoparticles labeled with Cy7, a near-infrared fluorescent compound, effectively accumulated in tumors (Fig. 4*D*, image on the left, arrow), with a significant signal from the liver as well (arrowhead). The reduction in the tumor signal obtained with heparin (Fig. 4*D*, image on the right) appeared greater in the fluorescence measurements than the 50% value determined by SQUID, possibly because the concentrated signal from the clots enhanced optical detection of the fluorescence. These results suggest that the clotting induced by CREKA-SPIO provides a particular advantage in tumor imaging.

## Discussion

We describe a nanoparticle system that provides effective accumulation of the particles in tumors. The system is based on four elements: First, coating of the nanoparticles with a tumor-homing peptide that binds to clotted plasma proteins endows the particles with a specific affinity for tumor vessels (and tumor stroma). Second, decoy particle pretreatment prolongs the blood half-life of the particles and increases tumor targeting. Third, the tumor-targeted nanoparticles cause intravascular clotting in tumor blood vessels. Fourth, the intravascular clots attract more nanoparticles into the tumor, amplifying the targeting.

We chose a peptide with specific affinity for clotted plasma proteins as the targeting element for our nanoparticles. The interstitial spaces of tumors contain fibrin and proteins that become cross-linked to fibrin in blood clotting, such as fibronectin (13, 15). The presence of these products in tumors, but not in normal tissues, is thought to be a result of leakiness of tumor vessels, which allows plasma proteins to enter from the blood into tumor tissue, where the leaked fibrinogen is converted to fibrin by tissue procoagulant factors (13, 14). The clotting creates new binding sites that can be identified and accessed with synthetic peptides (15). The present results show that the CREKA-modified nanoparticles not only bind to blood and plasma clots but can also induce localized tumor clotting. The nature of the particle may not be important for this activity, because we found both CREKA-coated iron oxide nanoparticles and micron-sized CREKA-coated liposomes to cause clotting in tumor vessels. The mechanism by which CREKA-SPIO and CREKA-liposomes induce vascular clotting requires further study. We speculate that the binding of one or more clotting products by the CREKA-modified particles may shift the balance of clotting and clot dissolution in the direction of clot formation and that the presence of this activity at the surface of particles may facilitate contact-dependent coagulation.

Some nanomaterials are capable of triggering systemic thrombosis (27), but, here, the thrombosis induced by the CREKA particles was confined to tumor vessels. The high concentration of the targeted particles in tumor vessels partially explains the selective localization of the thrombosis to tumor vessels. However, because no detectable clotting was seen in the liver, where the nanoparticles also accumulate at high concentrations, other factors must be important. The procoagulant environment common in tumors is likely to be a major factor contributing to the tumor-specificity of the clotting (28). It remains to be seen whether CREKA particles might bind to other regions of pathological clotting activity in the body (e.g., wounds) and to induce additional clotting at such sites.

A major advantage of nanoparticles is that multiple functions can be incorporated onto a single entity. We describe here an *in vivo* function for nanoparticles that has not been described previously; self-amplifying tumor homing enabled by nanoparticle-induced clotting in tumor vessels and the binding of additional nanoparticles to the clots. Our nanoparticle system combines several other functions into one particle: specific tumor homing, avoidance of the RES, and effective tumor imaging. We used optical imaging in this work, but the SPIO platform also enables MRI imaging, which does not suffer from the tissue-penetration problems that limit optical imaging in animals larger than mice and in humans. The clotting caused by CREKA-SPIO nanoparticles in tumor vessels serves to focally concentrate the particles in a manner that appears to improve tumor detection by microscopic and whole-body imaging techniques.

Another possibly useful function of our targeted particles is that they cause physical blockade of tumor vessels by local embolism. Blood vessel occlusion by embolism or clotting can reduce tumor growth (29, 30).To date, we have achieved a 20% occlusion rate in tumor vessels. Preliminary tumor treatment

experiments (D.S., L.Z., and E.R., unpublished work) have indicated that this degree of vessel occlusion is not sufficient to reduce the rate of tumor growth. However, future optimization of the procedure may change that. Finally, because of the modular nature of nanoparticle design, the functions we describe here can be incorporated into particles with additional activities. We envision the design of drug-carrying nanoparticles that accumulate in tumor vessels and slowly release the drug payload while simultaneously occluding the vessels.

## Materials and Methods

**Phage Screening, Tumors, and Peptides.** *In vivo* screening of a peptide library with the general structure of $CX_7C$, where C is cysteine and X is any amino acid, was carried out as described (5) by using 65- to 75-day-old transgenic MMTV PyMT mice (31). These mice express the polyoma virus middle T antigen (MT) under the transcriptional control of the mouse mammary tumor virus (MMTV), leading to the induction of multifocal mammary tumors in 100% of carriers. MDA-MB-435 tumors in nude mice and peptide synthesis have been described (32, 33). B16F1 murine melanoma tumors were grown in fibrinogen null mice (34) and their normal littermates and were used when they reached 0.5–1 cm in size (15).

**Nanoparticles and Liposomes.** Amino group-functionalized dextran-coated superparamagnetic iron oxide nanoparticles (50-nm nanomag-D-SPIO; Micromod Partikeltechnologie, Rostock, Germany) were coupled with CREKA peptide by using a cross-linker. The final coupling ratio was 30 nmol of fluorescein-labeled peptide molecules per milligram of iron oxide, or 8,000 peptides per particle. For near-infrared labeling with Cy7, ≈20% of the amines were derivatized with Cy7-NHS ester (GE Healthcare Bio-Sciences, Piscataway, NJ), and the remaining amines were used for conjugating the peptide. Details on the SPIO and the preparation of liposomes are described in *SI Materials and Methods*. Clodronate was purchased from Sigma (St. Louis, MO) and incorporated into liposomes as described (19).

**Nanoparticle Injections.** For i.v. injections, the animals were anesthetized with i.p. Avertin, and liposomes (2 $\mu$mol of DSPC) and/or nanoparticles (1–4 mg of Fe per kg of body weight) were injected into the tail vein. The animals were killed 5–24 h after injection by cardiac perfusion with PBS under anesthesia, and organs were dissected and analyzed for particle homing. To suppress liver macrophages, mice were intravenously injected with liposomal clodronate suspension (100 $\mu$l per mouse), and the mice were used for experiments 24 h later. All animal work was reviewed and approved by the Burnham Institute's Animal Research Committee.

**Phage and Nanoparticle Binding to Clots.** Phage binding to clotted plasma proteins was determined as described (15). CREKA-SPIO and control SPIO were added to freshly formed plasma clots in the presence or absence of free CREKA peptide. After 10 min of incubation, the clots were washed four times in PBS, transferred to a new tube and digested in 100 $\mu$l of concentrated nitric acid. The digested material was diluted in 2 ml of distilled water, and the iron concentration was determined by using inductively coupled plasma–optical emission spectroscopy (ICP-OES; PerkinElmer, Norwalk, CT).

**Plasma Protein Binding to Nanoparticles, Particle Clearance from the Blood, Intravital Microscopy and Magnetic Measurements.** For information on plasma protein binding and the other methods, see *SI Materials and Methods*.

We thank Drs. Eva Engvall, Douglas Hanahan, and Zaverio Ruggeri for discussions and comments on the manuscript; Dr. Joseph Beechem (Invitrogen, Carlsbad, CA) for Alexa 647-labeled CREKA; and Dr. Venkata Ramana Kotamraju for peptide synthesis. This work was supported by National Institutes of Health Contract N01-CO-37117 and, in part, by National Cancer Institute Grants CA119335 (to E.R., S.B., and M.J.S.) and CA099258 (to R.M.H.).

1. Desai N, Trieu V, Yao Z, Louie L, Ci S, Yang A, Tao C, De T, Beals B, Dykes D, *et al.* (2006) *Clin Cancer Res* 12:1317–1324.
2. Weissleder R, Bogdanov A, Jr, Neuwelt EA, Papisov M (1995) *Adv Drug Delivery Rev* 16:321–334.
3. Sinek J, Frieboes H, Zheng X, Cristini V (2004) *Biomed Microdevices* 6:297–309.
4. Boucher Y, Baxter LT, Jain RK (1990) *Cancer Res* 50:4478–4484.
5. Hoffman JA, Giraudo E, Singh M, Zhang L, Inoue M, Porkka K, Hanahan D, Ruoslahti E (2003) *Cancer Cell* 4:383–391.
6. Oh P, Li Y, Yu J, Durr E, Krasinska KM, Carver LA, Testa JE, Schnitzer JE (2004) *Nature* 429:629–635.
7. Ruoslahti E (2002) *Nat Rev Cancer* 2:83–90.
8. DeNardo SJ, DeNardo GL, Miers LA, Natarajan A, Foreman AR, Gruettner C, Adamson GN, Ivkov R (2005) *Clin Cancer Res* 11:7087s–7092s.
9. Akerman ME, Chan WC, Laakkonen P, Bhatia SN, Ruoslahti E (2002) *Proc Natl Acad Sci USA* 99:12617–12621.
10. Cai W, Shin DW, Chen K, Gheysens O, Cao Q, Wang SX, Gambhir SS, Chen X (2006) *Nano Lett* 6:669–676.
11. Pasqualini R, Ruoslahti E (1996) *Nature* 380:364–366.
12. Hutchinson JN, Muller WJ (2000) *Oncogene* 19:6130–6137.
13. Dvorak HF, Senger DR, Dvorak AM, Harvey VS, McDonagh J (1985) *Science* 227:1059–1061.
14. Abe K, Shoji M, Chen J, Bierhaus A, Danave I, Micko C, Casper K, Dillehay DL, Nawroth PP, Rickles FR (1999) *Proc Natl Acad Sci USA* 96:8663–8668.
15. Pilch J, Brown DM, Komatsu M, Jarvinen TA, Yang M, Peters D, Hoffman RM, Ruoslahti E (2006) *Proc Natl Acad Sci USA* 103:2800–2804.
16. Jung CW, Jacobs P (1995) *Magn Reson Imaging* 13:661–674.
17. Jung CW (1995) *Magn Reson Imaging* 13:675–691.
18. Weissleder R, Stark DD, Engelstad BL, Bacon BR, Compton CC, White DL, Jacobs P, Lewis J (1989) *Am J Roentgenol* 152:167–173.
19. Van Rooijen N, Sanders A (1994) *J Immunol Methods* 174:83–93.
20. Moghimi SM, Hunter AC, Murray JC (2001) *Pharmacol Rev* 53:283–318.
21. Moore A, Weissleder R, Bogdanov A, Jr (1997) *J Magn Reson Imaging* 7:1140–1145.
22. Souhami RL, Patel HM, Ryman BE (1981) *Biochim Biophys Acta* 674:354–371.
23. Fernandez-Urrusuno R, Fattal E, Rodrigues JM, Jr, Feger J, Bedossa P, Couvreur P (1996) *J Biomed Mater Res* 31:401–408.
24. Radomski A, Jurasz P, Alonso-Escolano D, Drews M, Morandi M, Malinski T, Radomski MW (2005) *Br J Pharmacol* 146:882–893.
25. Khandoga A, Stampfl A, Takenaka S, Schulz H, Radykewicz R, Kreyling W, Krombach F (2004) *Circulation* 109:1320–1325.
26. Van der Heyde HC, Gramaglia I, Sun G, Woods C (2005) *Blood* 105:1956–1963.
27. Gorbet MB, Sefton MV (2004) *Biomaterials* 25:5681–5703.
28. Boccaccio C, Sabatino G, Medico E, Girolami F, Follenzi A, Reato G, Sottile A, Naldini L, Comoglio PM (2005) *Nature* 434:396–400.
29. Huang X, Molema G, King S, Watkins L, Edgington TS, Thorpe PE (1997) *Science* 275:547–550.
30. El-Sheikh A, Borgstrom P, Bhattacharjee G, Belting M, Edgington TS (2005) *Cancer Res* 65:11109–11117.
31. Hutchinson JN, Muller WJ (2000) *Oncogene* 19:6130–6137.
32. Laakkonen P, Porkka K, Hoffman JA, Ruoslahti E (2002) *Nat Med* 8:751–755.
33. Laakkonen P, Akerman ME, Biliran H, Yang M, Ferrer F, Karpanen T, Hoffman RM, Ruoslahti E (2004) *Proc Natl Acad Sci USA* 101:9381–9386.
34. Suh TT, Holmback K, Jensen NJ, Daugherty CC, Small K, Simon DI, Potter S, Degen JL (1995) *Genes Dev* 9:2020–2033.